applied sciences

MDPI

Article

Systematic Analysis of Ultrasound Parameters for Gene Delivery Efficiency and Cell Viability in 4T1 Cells

Kichang Shin [1,†], Mi Jeong Kim [2,†], Jiwon Jeong [3], Sunjoo Jeong [3] and Hak Jong Lee [1,2,4,5,6,*]

[1] Department of Health Science and Technology, Graduate School of Convergence Science and Technology, Seoul National University, Seoul 08826, Republic of Korea; skc5027@snu.ac.kr
[2] Department of Radiology, Seoul National University Bundang Hospital, Seongnam-si 13620, Republic of Korea; mjekim1@gmail.com
[3] RNA Cell Biology Lab, Next-Generation RNA Editing Technology Center, Department of Bioconvergence Engineering, Dankook University Graduate School, Yongin-si 16890, Republic of Korea; jw_0916@naver.com (J.J.); sjsj@dankook.ac.kr (S.J.)
[4] Department of Medical Device Development, Seoul National University College of Medicine, Seoul 03080, Republic of Korea
[5] Department of Radiology, Seoul National University College of Medicine, Seoul 03080, Republic of Korea
[6] Institute of Radiation Medicine, Seoul National University Medical Research Center, Seoul 03080, Republic of Korea
* Correspondence: hakjlee@snu.ac.kr
† These authors contributed equally to this work.

Abstract

Gene therapy is a promising strategy for treating various diseases. However, its application remains limited by inefficient intracellular delivery, particularly in difficult-to-transfect cells such as triple-negative breast cancer (TNBC). Ultrasound-mediated gene delivery has emerged as a non-invasive approach to enhance membrane permeability, but its efficiency and safety depend strongly on acoustic parameters. In this study, we systematically investigated the effects of ultrasound intensity, pulse repetition frequency (PRF), duty cycle, and exposure time on gene delivery efficiency and cytotoxicity in 4T1 murine TNBC cells using microbubble-mediated sonoporation. Gene expressions were evaluated using a luciferase assay, and cell viability was assessed using an MTT assay. Total acoustic energy was calculated to analyze the relationship between cumulative ultrasound exposure and biological responses. Increasing total acoustic energy was associated with enhanced gene expression and reduced cell viability. However, gene expression increased only up to a certain level and then showed no further substantial increase, whereas cell viability continued to decline. Parameter-specific analysis further indicated that biological responses were not determined by total acoustic energy alone. These findings suggest that both cumulative acoustic energy and individual ultrasound parameters should be considered when optimizing ultrasound-mediated gene delivery to balance transfection efficiency and cytotoxicity.

Keywords: ultrasound; gene delivery; acoustic parameters; microbubbles

Academic Editor: Arkady Voloshin

Received: 28 May 2026
Revised: 20 June 2026
Accepted: 22 June 2026
Published: 30 June 2026

1. Introduction

Gene therapy has gained increasing attention as a promising approach for the treatment of a wide range of diseases, including cancer, genetic disorders, and regenerative conditions [1,2]. By delivering therapeutic nucleic acids into target cells, gene therapy enables precise regulation of cellular functions. However, the successful application of

gene therapy remains limited by the lack of efficient and safe delivery systems capable of overcoming the inherently low permeability of the cellular membrane to macromolecules, which restricts intracellular delivery of nucleic acids [3,4].

In particular, this limitation becomes more pronounced in certain cancer cell types, such as triple-negative breast cancer (TNBC), which are considered difficult to transfect due to their low membrane permeability and intrinsic resistance to intracellular uptake of macromolecules [5–7]. As a result, the effectiveness of conventional non-viral gene delivery approaches, including lipid-based and polymer-based carriers, is significantly reduced, as these systems largely rely on endocytosis-dependent mechanisms [8–10]. Therefore, strategies that can enhance membrane permeability in a controlled and non-invasive manner are required to improve intracellular gene delivery efficiency.

Ultrasound-mediated gene delivery, also known as sonoporation, has emerged as a promising physical method to overcome these limitations [11–13]. Ultrasound can induce mechanical effects, particularly cavitation, which temporarily disrupts the cell membrane and allows exogenous molecules such as plasmid DNA to enter the cytoplasm [14–16]. The use of microbubbles (MBs) further enhances this effect by amplifying cavitation activity under ultrasound exposure, thereby significantly improving transfection efficiency [17,18].

Despite these advantages, the efficiency and safety of ultrasound-mediated gene delivery remain highly dependent on acoustic parameters, including intensity, pulse repetition frequency (PRF), duty cycle, and exposure time [19,20]. While higher acoustic energy can enhance membrane permeabilization and gene uptake, it may also induce excessive mechanical stress, leading to cell damage or death [21,22]. Conversely, insufficient acoustic stimulation may result in poor transfection efficiency [23]. Thus, a critical challenge in this field is to systematically understand how ultrasound parameters influence gene delivery outcomes and cellular viability.

In this study, we systematically investigated the effects of ultrasound parameters on gene delivery efficiency and cytotoxicity in 4T1 murine TNBC cells using MB-mediated sonoporation. By analyzing relationships between ultrasound parameters and biological responses, we aimed to evaluate how acoustic variables influence transfection outcomes and cellular viability.

2. Materials and Methods

2.1. Acoustic Field Characterization and MI-Based Selection of Ultrasound Exposure Conditions

As illustrated in Figure 1a, ultrasound was irradiated from beneath the well plate, and the peak negative pressure might be attenuated due to the presence of the well plate. To evaluate this ultrasonic attenuation, the pressure was measured with the well plate. The ultrasonic device, a sonoporator (SP100, Sonidel Ltd., Dublin, Ireland), was used, and the pressure was measured by varying the intensity displayed on the sonoporator. The signal processing is detailed as follows. The pressure generated by the transducer was converted into an electrical signal using a hydrophone (4206, Precision Acoustics Ltd., Dorchester, UK). This signal was subsequently measured on an oscilloscope (DPO4104, Tektronix Inc., Beaverton, OR, USA) through a DC coupler (DCPS950, Precision Acoustics Ltd.). The acquired signal was then processed and visualized to determine intensity distributions in both one-dimensional (1D) and two-dimensional (2D) formats using MATLAB (version 26.1, R2026a; MathWorks, Natick, MA, USA).

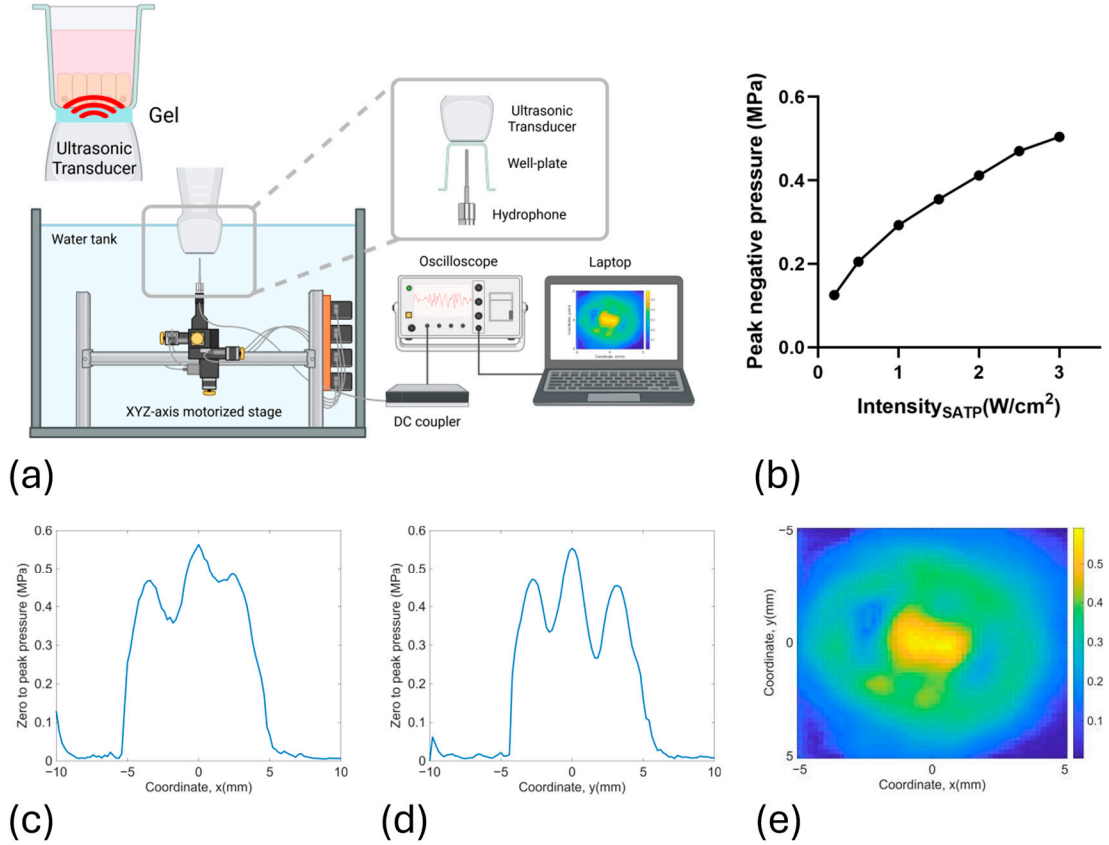

Figure 1. Schematic of the ultrasound setup and pressure distribution with a well plate. (**a**) Experimental setup for acoustic pressure measurement (created with BioRender.com). (**b**) Graph of peak negative pressure values as a function of spatial-average temporal peak intensity (I_{SATP}) with well plate. (**c**,**d**). One-dimensional acoustic pressure distributions along the x-axis (**c**) and y-axis (**d**), respectively, at 5 W/cm^2 intensity with well plate. (**e**) Two-dimensional acoustic pressure distributions at 5 W/cm^2 intensity with well plate.

To define appropriate ultrasound exposure conditions for subsequent gene delivery experiments, the ultrasound intensity range was selected based on the calculated mechanical index (MI). Detailed information on MI calculation is provided in the Supplementary Materials.

2.2. Preparation of Microbubbles

The overall MB structure is illustrated in Figure 2a. MBs were prepared using the thin-film hydration method. 1,2-distearoyl-sn-glycero-3-phosphocholine (DSPC) (Lipoid GmbH, Ludwigshafen, Germany) and N-(Methylpolyoxyethylene oxycarbonyl)-1,2-distearoyl-sn-glycero-3-phosphoethanolamine (DSPE-PEG 2000) (NOF Corporation, Tokyo, Japan) were dissolved in 100 µL of chloroform (Daejung Chemicals & Metals Co., Ltd., Siheung-si, Republic of Korea) at a 9:1 molar ratio, with a total lipid mass of 1 mg. The chloroform was evaporated overnight to form a thin phospholipid film. The completely dried thin film was hydrated using 1 mL of Dulbecco's Phosphate-Buffered Saline (DPBS) without calcium and magnesium (Biowest, Nuaillé, France) to reach a final lipid concentration of 1 mg/mL. During hydration, the vial containing the lipid film and DPBS was immersed in a 56 °C water bath and sonicated using an ultrasonic bath sonicator (JAC-5020; KODO Technical Research Co., Ltd., Hwaseong-si, Republic of Korea). This cycle was repeated three times to ensure complete dispersion of the phospholipid film. The headspace of the vial was then replaced with sulfur hexafluoride gas (SF_6) for 45 s. Finally, the vials were agitated using a Vialmix™ shaker (Bristol-Myers Squibb, New York, NY, USA) for 45 s to generate MBs.

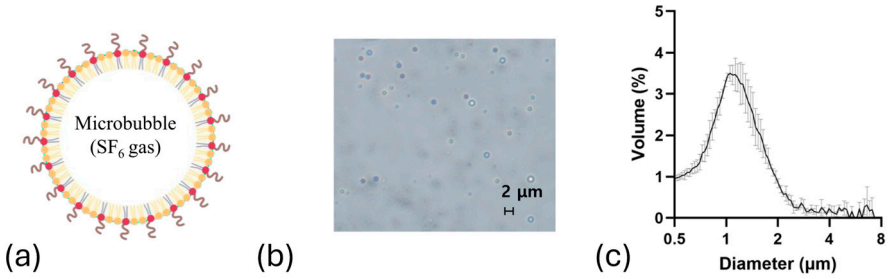

Figure 2. Schematic representation and characterization of microbubbles. (**a**) Schematic illustration of a microbubble composed of a phospholipid shell and sulfur hexafluoride (SF_6) gas core (created with BioRender.com). In the schematic, red indicates DSPE-PEG2000 and yellow indicates DSPC. (**b**) Optical microscopic image of synthesized microbubbles (scale bar = 2 μm). (**c**) Size distribution of microbubbles measured using a Coulter Counter, showing a peak diameter around 1.4 μm.

2.3. Cell Culture

Murine mammary carcinoma (4T1) cells were grown in RPMI 1640 with glutamine (Biowest, Bradenton, FL, USA) supplemented with 10% heat-inactivated fetal bovine serum (FBS) (Biowest), 100 U/mL penicillin (Gibco, Grand Island, NY, USA), and 100 μg/mL streptomycin (Gibco). Cells were cultured in a 5% CO_2 humidified atmosphere at 37 °C.

2.4. Plasmid

We constructed luciferase reporters containing the β-catenin 3′ untranslated region (3′UTR-2, 752nt). The β-catenin 3′UTR-2 was amplified in cDNA synthesized from SW480 cell-derived RNA. PCR was carried out using Pfu DNA polymerase (Thermo Fisher Scientific, Waltham, MA, USA; #EP0501) and XbaI-tailed primers: forward 5′-AAATCTAGAATCATCCTTTAGGTAAGAAG-3′ and reverse 5′-AAATCTAGAGAATGAATTAAAAGTTTAATTC-3′. The amplified β-catenin 3′UTR-2 was cloned into the XbaI restriction enzyme site of pZeo/Luc vector (a kind gift from Dr. Stephen M. Prescott). For in vitro transfection experiments, endotoxin-free plasmid DNA of the pZeo/Luc+β-catenin 3′UTR-2 was prepared using the NucleoBond Xtra Midi EF kit (MACHEREY-NAGEL, #740420.50, Düren, Germany), following the manufacturer's protocol.

2.5. In Vitro Ultrasound-Mediated Gene Delivery

The ultrasound parameters used in this study, including intensity, PRF, duty cycle, and exposure time, are illustrated in Figure 3. Intensity represents the amplitude of acoustic pressure, PRF determines the repetition rate of pulses, duty cycle defines the fraction of time during which ultrasound is actively delivered within each cycle, and exposure time corresponds to the total duration of ultrasound application.

Based on these parameters, the experimental procedure for ultrasound-mediated gene delivery is schematically depicted in Figure 4a. 4T1 cells were seeded at 2×10^4 cells/well in the 24-well plates, every second row and column, to prevent interaction of ultrasound irradiation. After 24 h incubation, each medium in the well was removed, and media (500 μL) with plasmid DNA (0.5 μg) and MBs (50 μL) were added to each well. The cells were then exposed to ultrasound using the sonoporator. Ultrasound parameters varied by changing the intensity, PRF, duty cycle, and exposure time. The control group consisted of untreated 4T1 cells without plasmid DNA, MBs, or ultrasound irradiation. Additional baseline control groups, including DNA alone, DNA + MB, and DNA + US, were evaluated and are presented in the Supplementary Materials. Each group was conducted with n = 4. At 6 h after ultrasound irradiation treatment, the media in the wells were replaced with new medium. The cells were incubated at 37 °C for 18 h before the in vitro luciferase assay and MTT assay.

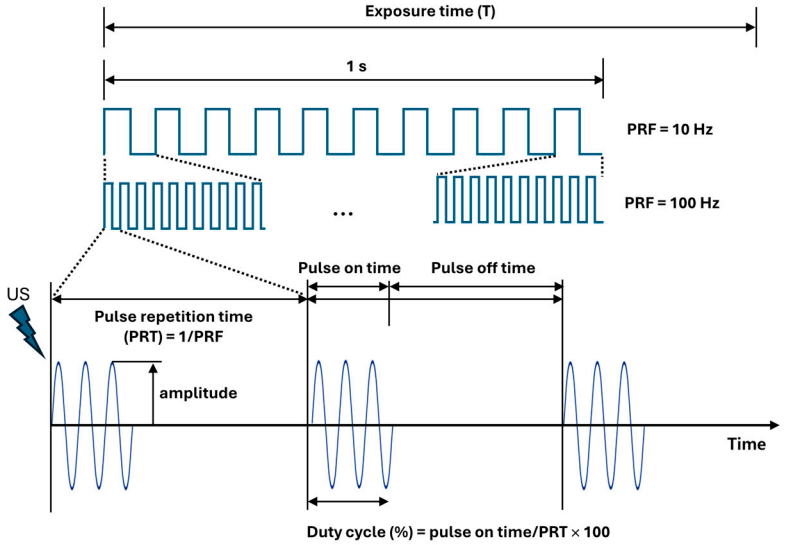

Figure 3. Schematic illustration of ultrasound exposure parameters. Acoustic intensity, PRF, duty cycle, and exposure time were used to define ultrasound exposure conditions.

2.6. Luciferase Assay

For luciferase activity measurements, the cells were lysed in the lysis buffer (Luciferase Cell Culture Lysis 5× Reagent, Promega, Madison, WI, USA), and the cell lysate was moved to the 96-well plate. Luciferase activity was measured using a luciferase assay system (Dual-glo® Luciferase Assay System, Promega) and a multi-mode microplate reader (SpectraMax iD3, Molecular Devices, San Jose, CA, USA). To minimize the influence of differences in cell viability among treatment conditions, luciferase activity was normalized to the total protein amount of each well. The total protein amount of each well was measured using a BCA protein assay system (Pierce™ BCA Protein Assay Kit, Thermo Fisher Scientific, Rockford, IL, USA) and the multi-mode microplate reader. Luciferase activity is reported as the mean of relative light units (RLUs) per mg protein obtained from each well.

2.7. Cytotoxicity Assay

To assess the effects of ultrasound irradiation on cell viability, an MTT (3-(4,5-dimethylthiazol-2-yl)-2,5-diphenyltetrazolium bromide, a tetrazole) assay was performed. After 24 h post-ultrasound irradiation treatment, 12 mM MTT (Invitrogen, Eugene, OR, USA) dissolved in PBS was added to the cells (50 µL/well), and the cells were incubated at 37 °C for 4 h. Then, 100 µL of the SDS-HCl solution was added to each well. After 4 h in a humidified chamber, the cells were moved to the 96-well plate, and the absorbance at 570 nm of each well was measured using the multi-mode microplate reader.

2.8. Analysis of Total Acoustic Energy

To further analyze the relationship between ultrasound exposure conditions and biological responses, total acoustic energy was calculated based on the applied ultrasound settings. Ultrasound exposure consisted of pulsed sonication defined by acoustic intensity (I), pulse repetition frequency (PRF), duty cycle (DC), and exposure time (T) (Figure 3).

The total acoustic energy delivered during treatment was calculated as:

$$\text{Total acoustic energy } = \text{I} \times \text{DC} \times \text{T}$$

For total acoustic energy calculations, duty cycle was converted from percentage to fractional form by dividing by 100, allowing the resulting value to be expressed in J/cm^2. This parameter represents the cumulative acoustic energy delivered to the target during

sonication. To evaluate the relationship between each ultrasound parameter and total acoustic energy, experiments were performed by varying a single parameter while keeping all other acoustic conditions constant. This approach enabled independent assessment of the effect of each experimental variable on the resulting total acoustic energy.

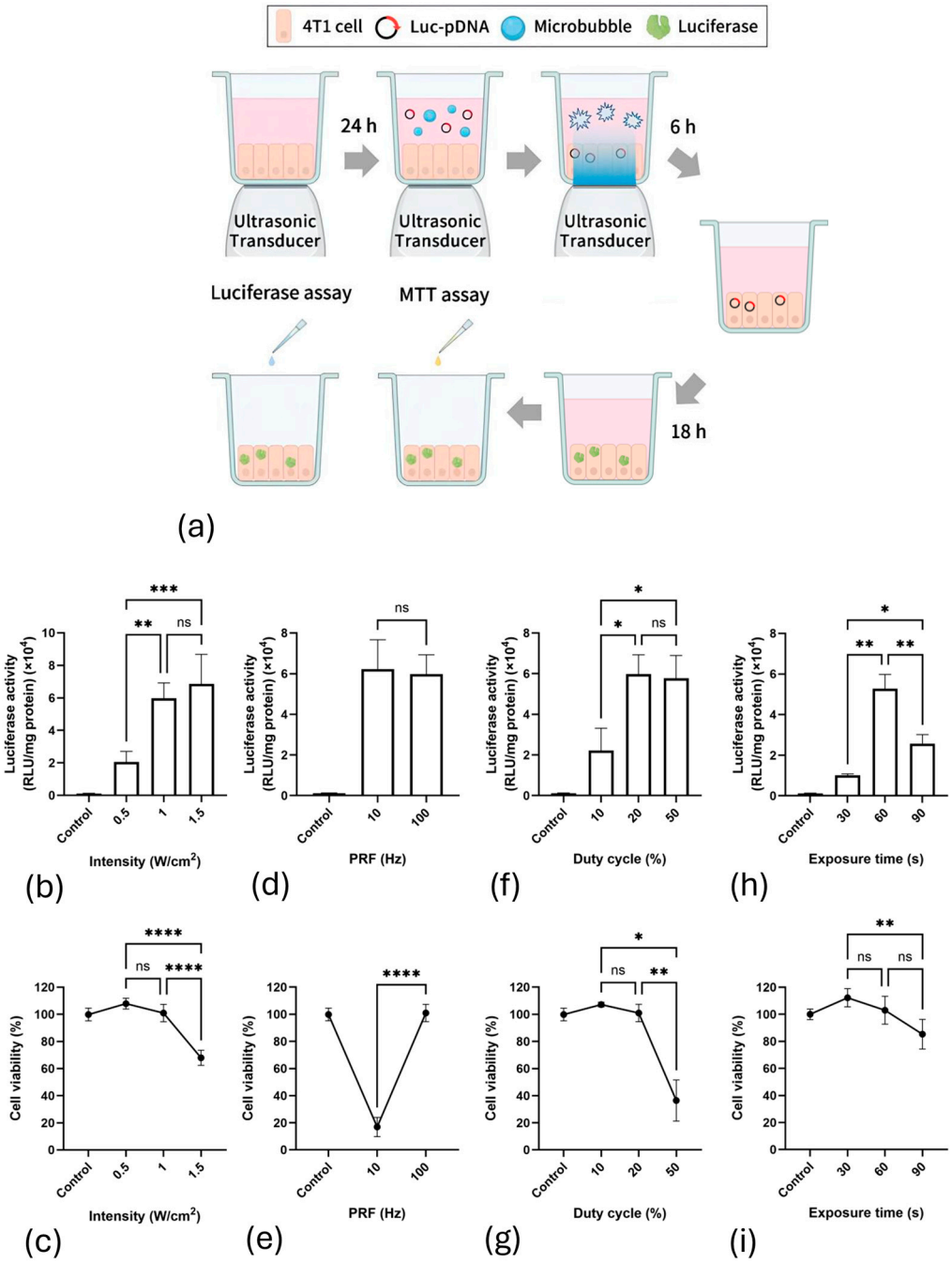

Figure 4. Gene transfection efficiency and cell viability under different ultrasound parameters. (**a**) Schematic representation of methods of in vitro ultrasound-mediated gene delivery and analysis in a 24-well plate (created with BioRender.com). Effect of acoustic intensity (0.5, 1, and 1.5 W/cm^2) on luciferase expression (**b**) and cell viability (**c**). Effect of pulse repetition frequency (PRF, 10 and 100 Hz) on luciferase expression (**d**) and cell viability (**e**). Effect of duty cycle (10%, 20%, and 50%) on luciferase expression (**f**) and cell viability (**g**). Effect of ultrasound exposure time (30, 60, and 90 s) on luciferase expression (**h**) and cell viability (**i**). Luciferase activity is presented as relative light units (RLU) per mg protein, and cell viability is expressed as a percentage of control. Data are presented as mean ± SD (n = 4). * $p < 0.05$, ** $p < 0.01$, *** $p < 0.001$, **** $p < 0.0001$; ns, not significant.

2.9. Statistical Analysis

All in vitro data were expressed as mean ± SD. Statistical significance between groups was determined using one-way ANOVA followed by Tukey's HSD test. Statistical significance was defined as $p < 0.05$. All analyses were performed using GraphPad Prism (v9.4, GraphPad Software, Inc., San Diego, CA, USA).

3. Results

3.1. Assessment of Ultrasound Attenuation by the Well Plate

To evaluate the efficiency of gene transfer induced by ultrasound irradiation, we cultured cells on a well plate and applied ultrasound from the bottom of the plate. Ultrasound penetrates the culture plate to reach the cells. Therefore, we examined whether the presence of a well plate affected ultrasound attenuation (Figure 1a). Figure 1b shows the peak negative pressure measured depending on the intensity of the sonoporator. The results demonstrated that the peak negative pressure increased dependently with increasing intensity. The detailed acoustic pressure and corresponding MI values are summarized in Table S1.

The mechanical index (MI) was calculated from the measured acoustic pressure and the transducer center frequency to evaluate cavitation potential. Previous studies have shown that MI values between 0.05 and 0.2 do not significantly affect MB concentration, values in the range of 0.2–0.3 increase to compression relative to expansion, and values above 0.3 lead to a rapid decrease in the MB population [24–26]. Considering these observations, ultrasound intensities of 0.5, 1, and 1.5 W/cm^2 corresponding to MI values of 0.205, 0.293, and 0.355, respectively, were selected as parameter conditions for subsequent gene delivery experiments. Analysis of the pressure field showed that the pressure became concentrated towards the center region, resulting in locally elevated peak pressure values (Figure 1c–e).

3.2. Characterization of Microbubbles

As shown in Figure 2b, the synthesized MBs exhibited a uniform spherical morphology. The size distribution and number of MBs were measured using a Coulter Counter (Multisizer 4e, Beckman Coulter, Brea, CA, USA) (Figure 2c). The average size of the synthesized MBs was 1.413 ± 0.246 μm. The number of MBs was $9.97 \times 10^{10} \pm 4.94 \times 10^{9}$/mL.

3.3. In Vitro Optimization of US-Mediated Gene Transfer

Before evaluating the effects of individual ultrasound parameters, we first examined baseline control conditions, including untreated control, DNA alone, DNA + MB, and DNA + US groups. No significant differences in luciferase activity or cell viability were observed among these groups, indicating that DNA, MBs, or ultrasound alone did not substantially affect reporter expression or cell viability under the tested conditions (Figure S1). Based on these baseline results, we next evaluated the effects of ultrasound (US) parameters on gene transfection efficiency and cell viability in 4T1 cells using luciferase-expressing plasmid DNA (pZEO luc 3′UTR-2) in combination with MBs. Luciferase activity was measured 24 h after ultrasound exposure, while cell viability was assessed using the MTT assay. The effects of each parameter on gene transfection efficiency and cell viability are shown in Figure 4.

To determine the optimal acoustic intensity, cells were exposed to ultrasound at a center frequency of 1 MHz, PRF of 100 Hz, duty cycle of 20%, and exposure time of 60 s, while varying the acoustic intensity from 0.5 to 1.5 W/cm^2. As shown in Figure 4b, luciferase activity significantly increased with increasing acoustic intensity. The highest transfection efficiency was observed with 1.5 W/cm^2, showing approximately 3-fold higher luciferase activity compared with 0.5 W/cm^2. However, increased acoustic intensity also resulted

in marked cytotoxicity (Figure 4c). In particular, cell viability dramatically decreased at 1.5 W/cm^2, reaching below 30% of the control group, indicating that excessive acoustic exposure induced cellular damage.

The effect of PRF on gene transfection efficiency and cell viability is shown in Figure 4d,e. Cells were irradiated with ultrasound at a center frequency of 1 MHz, an intensity of 1 W/cm^2, a duty cycle of 20%, and an exposure time of 60 s. Although no significant difference in luciferase activity was observed between PRF conditions (Figure 4d), cell viability decreased with decreasing PRF (Figure 4e). When the PRF was 10 Hz, the cell viability was lower than 20%.

The ultrasound parameters were fixed at a center frequency of 1 MHz, an intensity of 1 W/cm^2, a PRF of 100 Hz, and an exposure time of 60 s, except for the duty cycle. At a 20% duty cycle, luciferase activity reached $5.9 \times 10^4 \pm 9.8 \times 10^3$ RLU/mg protein, which was higher than at 10% and comparable to that at 50% (Figure 4f). As shown in Figure 4g, increasing the duty cycle from 10% to 50% resulted in a significant decrease in cell viability.

The influence of ultrasound exposure time on transfection efficiency and cell viability is shown in Figure 4h,i. Cells were exposed to ultrasound at a center frequency of 1 MHz, an intensity of 1 W/cm^2, a PRF of 100 Hz, and a duty cycle of 20%. An exposure time of 60 s resulted in higher gene expression than 30 or 90 s (Figure 4h). Meanwhile, cell viability showed a significant decrease with the increase in ultrasound exposure time (Figure 4i).

3.4. Relationship Between Total Acoustic Energy and Biological Responses

To further investigate the relationship between ultrasound exposure conditions and biological responses, total acoustic energy was calculated based on the applied ultrasound settings. The ultrasound conditions used to calculate total acoustic energy are summarized in Supplementary Tables S2–S4. PRF was fixed at 100 Hz, while intensity, duty cycle, and exposure time were varied to generate total acoustic energy values of 6, 12, 18, and 30 J/cm^2.

As shown in Figure 5a, luciferase expression increased significantly as total acoustic energy increased from 6 to 12 J/cm^2. At higher energy levels of 18 and 30 J/cm^2, luciferase activity remained relatively constant, with no further substantial increase observed. Cell viability (Figure 5b) showed a gradual decrease between 6 and 12 J/cm^2, followed by a sharp decline at higher energy levels. At 18 J/cm^2, viability dropped noticeably, and a substantial reduction was observed at 30 J/cm^2, where cell viability fell below 40%.

To further compare whether the biological responses differed depending on which ultrasound parameter was varied to generate the same total acoustic energy, the effects of intensity, duty cycle, and exposure time were analyzed separately (Figure 5c,d). As shown in Figure 5c, luciferase expression generally increased as total acoustic energy increased from 6 to 12 J/cm^2 regardless of the ultrasound parameter adjusted. However, the response patterns diverged at higher energy levels. When total acoustic energy was increased by changing intensity or duty cycle, luciferase expression was maintained or slightly increased at higher energy levels, whereas increasing exposure time resulted in reduced luciferase expression at 18 J/cm^2. In contrast, cell viability decreased as total acoustic energy increased regardless of the parameter (Figure 5d). These findings suggest that although total acoustic energy is associated with both gene expression and cytotoxicity, the biological outcome may also depend on how this energy is delivered through individual ultrasound parameters.

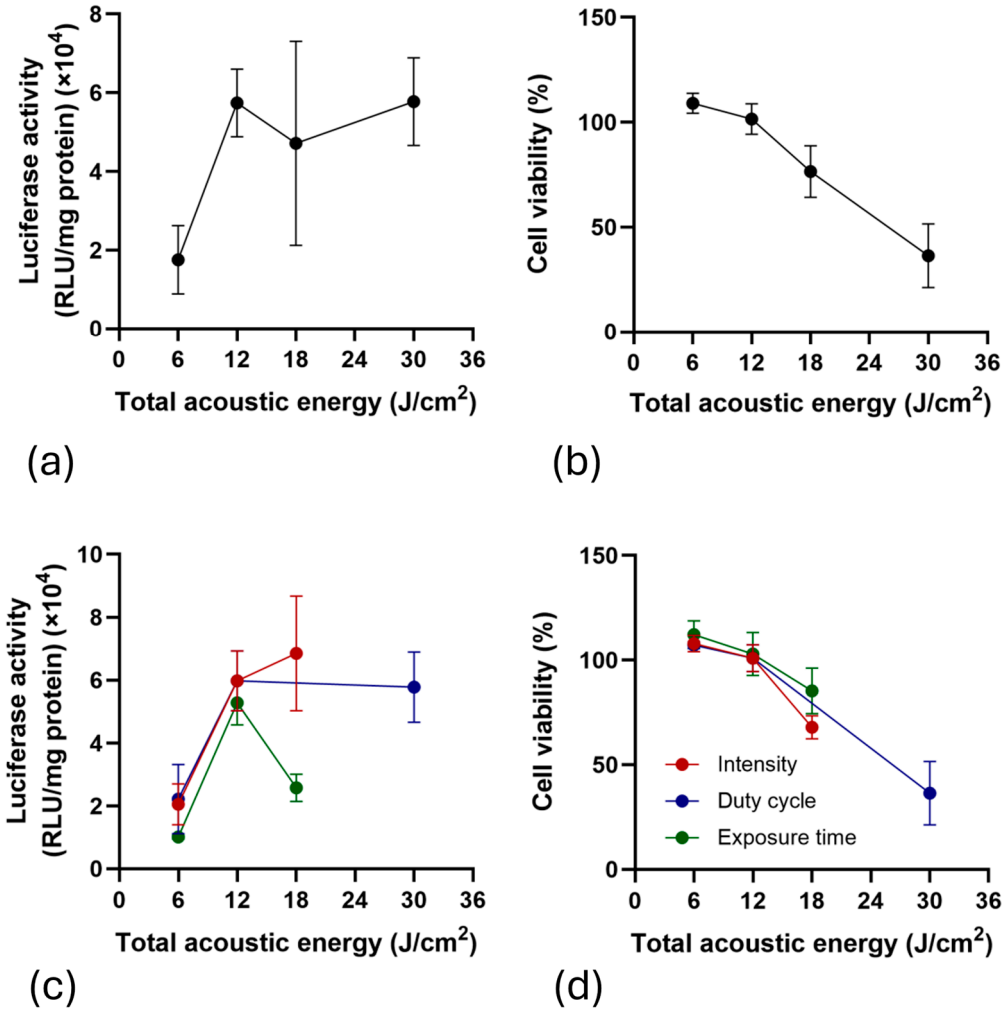

Figure 5. Effects of total acoustic energy on ultrasound-mediated gene expression and cell viability. Luciferase expression (**a**) and cell viability (**b**) according to the total acoustic energy. Parameter-specific effects of total acoustic energy generated by changes in intensity, duty cycle, and exposure time on luciferase expression (**c**) and cell viability (**d**).

4. Discussion

This study systematically evaluated the effects of ultrasound parameters on gene delivery efficiency and cytotoxicity in 4T1 murine TNBC cells using MB-mediated sonoporation. The results demonstrate that ultrasound-mediated gene delivery is strongly influenced by acoustic conditions, including intensity, PRF, duty cycle, and exposure time, which collectively determine both transfection efficiency and cellular viability.

Prior to assessing biological responses, the potential influence of the well plate on acoustic propagation was examined. The presence of the well plate resulted in a non-uniform acoustic field, with acoustic pressure concentrated toward the central region. Although this spatial heterogeneity was observed, the measured acoustic pressure increased consistently with the applied intensity, following the expected relationship between intensity and pressure ($I \propto p^2$) [27], as confirmed by a strong correlation ($R^2 = 0.998$). This indicates that the overall acoustic pressure was reliably controlled across conditions, despite local variations in the spatial distribution of the acoustic field.

Systematic evaluation of ultrasound parameters revealed that increasing intensity significantly enhanced gene expression while simultaneously decreasing cell viability. The stronger acoustic pressure at higher intensities induces enhanced cavitation, which in turn intensifies MB dynamics [28]. These dynamic effects exert greater mechanical forces

on the cell membrane, leading to increased membrane permeabilization. However, such increased mechanical stress can also disrupt membrane structure and interfere with cellular equilibrium, thereby contributing to reduced cell viability [29,30].

Likewise, lower PRF (10 Hz) induced more cell damage than the higher PRF (100 Hz), despite comparable levels of luciferase activity. This indicates that higher PRF, which corresponds to shorter and more frequent pulses under the same total exposure duration, may mitigate cellular damage by reducing the energy per acoustic event [31].

In addition to intensity and PRF, duty cycle and exposure time also played critical roles in balancing transfection efficiency and cell viability. Specifically, increasing the duty cycle from 20% to 50% led to a notable rise in cytotoxicity without a corresponding improvement in gene expression. This suggests that a higher duty cycle, which extends the duration of each acoustic burst, may promote excessive mechanical stress on cells [32], outweighing any potential gains in transfection. In contrast, a 20% duty cycle provided a more favorable balance by enabling effective cavitation activity while limiting cumulative energy delivery.

Similarly, ultrasound exposure time exhibited a non-linear effect on transfection and cell viability. Increasing the duration from 30 to 60 s improved gene expression, but extending it to 90 s markedly reduced viability, likely due to sustained cavitation-induced stress. These results are consistent with previous studies showing that prolonged ultrasound exposure can enhance gene delivery but may also increase cellular damage, depending on the exposure time [33].

Notably, analysis of total acoustic energy provided additional insight into the relationship between ultrasound exposure and biological responses. Increasing total acoustic energy was generally associated with enhanced gene expression and reduced cell viability (Figure 5). Under conditions where PRF was fixed, higher total acoustic energy reflected greater overall acoustic input, mainly through increased acoustic intensity. Increased cumulative acoustic exposure may promote membrane permeabilization by sustaining ultrasound- and MB-induced mechanical effects over time, thereby facilitating intracellular plasmid delivery [34]. However, excessive acoustic exposure may also prolong cavitation-induced mechanical stress, resulting in cellular damage and reduced viability [35,36].

Importantly, total acoustic energy alone did not fully explain the biological outcomes observed in this study. Although total acoustic energy provides a useful measure of overall ultrasound exposure, different parameter combinations may generate distinct biological effects even at comparable energy levels [16]. This is because intensity, PRF, and duty cycle affect MB behavior in different ways. Acoustic intensity mainly determines the strength of MB oscillation and cavitation activity, thereby influencing the degree of membrane permeabilization and cavitation-induced mechanical stress [16,29,34]. In contrast, PRF and duty cycle are both time-dependent pulse parameters that regulate the temporal pattern of ultrasound exposure. By determining how frequently acoustic pulses are delivered and how long ultrasound remains active within each pulse cycle, these parameters can affect repeated MB activation, cavitation persistence, and the duration of cavitation-related mechanical effects [11,19]. Therefore, differences in pulse timing and active exposure duration may alter microstreaming, shear stress, and mechanical stimulation applied to cells, even when the total acoustic energy is comparable [34,37]. Thus, the biological response depends not only on the total acoustic energy delivered but also on the temporal and mechanical pattern by which that energy activates MBs and stresses the cell membrane.

Taken together, these findings suggest that optimization of ultrasound-mediated gene delivery should consider both cumulative acoustic energy and individual ultrasound parameters. Beyond a certain exposure level, additional acoustic energy may not proportionally improve gene delivery efficiency and may instead increase cytotoxicity. Therefore, effective optimization requires selection of acoustic conditions that induce sufficient mem-

brane permeabilization for gene transfer while minimizing excessive cavitation-related cellular damage.

5. Conclusions

This study demonstrates that ultrasound-mediated gene delivery in 4T1 murine TNBC cells is influenced by both cumulative acoustic energy and individual ultrasound parameters. Although increasing acoustic exposure can enhance gene delivery, excessive exposure reduces cell viability, highlighting the need to balance transfection efficiency and cytotoxicity. Importantly, total acoustic energy alone does not fully predict biological outcomes, as different parameter combinations can produce distinct effects at similar energy levels. These findings suggest that optimization of MB-mediated sonoporation should consider not only total acoustic energy but also how intensity, PRF, duty cycle, and exposure time individually affect gene delivery efficiency and cell viability. Together, these results provide a quantitative basis for selecting ultrasound conditions that improve gene delivery while preserving cell viability in difficult-to-transfect cancer cells.

Supplementary Materials: The following supporting information can be downloaded at: https://www.mdpi.com/article/10.3390/app16136500/s1, Method S1: Mechanical index calculation; Figure S1: Effects of baseline control groups on luciferase activity and cell viability; Table S1: Acoustic pressure and mechanical index (MI) at varying ultrasound intensities with a well plate; Table S2: Total acoustic energy calculations according to changes in acoustic intensity; Table S3: Total acoustic energy calculations according to changes in duty cycle; Table S4: Total acoustic energy calculations according to changes in exposure time.

Author Contributions: Conceptualization, M.J.K. and S.J.; methodology, K.S. and J.J.; software, K.S.; validation, K.S., M.J.K. and J.J.; formal analysis, K.S., M.J.K. and J.J.; investigation, K.S., M.J.K. and J.J.; resources, H.J.L.; data curation, K.S. and M.J.K.; writing—original draft preparation, K.S., M.J.K. and J.J.; visualization, K.S.; supervision, H.J.L. and S.J.; project administration, H.J.L.; funding acquisition, H.J.L. and S.J. All authors have read and agreed to the published version of the manuscript.

Funding: This work was supported by grant no. 13-2022-0003 and 18-2023-0010 from the Seoul National University Bundang Hospital (SNUBH) Research Fund. This work was supported by the National Research Foundation of Korea (NRF) grant funded by the Korea government (MSIT) [No. RS-2023-00208597] and [No. RS-2025-00561939].

Institutional Review Board Statement: Not applicable.

Informed Consent Statement: Not applicable.

Data Availability Statement: The data presented in this study are available from the corresponding author upon reasonable request.

Acknowledgments: Schematic illustrations were created with BioRender. This manuscript was partially edited for English language using ChatGPT based on GPT-4o (OpenAI, San Francisco, CA, USA), and all content was reviewed and approved by the authors. The authors are grateful to IMGT Co. for their technical assistance. The authors would like to thank Daeseung Kim and Minseok Kim from IMGT Co., Ltd. for their valuable assistance with the assessment of ultrasound attenuation.

Conflicts of Interest: The authors declare no conflicts of interest.

References

1. Dastjerd, N.T.; Valibeik, A.; Rahimi Monfared, S.; Goodarzi, G.; Moradi Sarabi, M.; Hajabdollahi, F.; Maniati, M.; Amri, J.; Samavarchi Tehrani, S. Gene therapy: A promising approach for breast cancer treatment. *Cell Biochem. Funct.* **2022**, *40*, 28–48. [PubMed]
2. Sheikh-Hosseini, M.; Larijani, B.; Gholipoor Kakroodi, Z.; Shokoohi, M.; Moarefzadeh, M.; Sayahpour, F.A.; Goodarzi, P.; Arjmand, B. Gene therapy as an emerging therapeutic approach to breast cancer: New developments and challenges. *Hum. Gene Ther.* **2021**, *32*, 1330–1345. [CrossRef] [PubMed]

3. Stewart, M.P.; Langer, R.; Jensen, K.F. Intracellular delivery by membrane disruption: Mechanisms, strategies, and concepts. *Chem. Rev.* **2018**, *118*, 7409–7531. [CrossRef] [PubMed]
4. Varkouhi, A.K.; Scholte, M.; Storm, G.; Haisma, H.J. Endosomal escape pathways for delivery of biologicals. *J. Control. Release* **2011**, *151*, 220–228. [CrossRef] [PubMed]
5. Wang, Y.; Tang, J.; Yang, Y.; Song, H.; Fu, J.; Gu, Z.; Yu, C. Functional nanoparticles with a reducible tetrasulfide motif to upregulate mRNA translation and enhance transfection in hard-to-transfect cells. *Angew. Chem.* **2020**, *132*, 2717–2721. [CrossRef]
6. Hur, J.; Park, I.; Lim, K.M.; Doh, J.; Cho, S.-G.; Chung, A.J. Microfluidic cell stretching for highly effective gene delivery into hard-to-transfect primary cells. *ACS Nano* **2020**, *14*, 15094–15106. [CrossRef] [PubMed]
7. Gresch, O.; Altrogge, L. Transfection of difficult-to-transfect primary mammalian cells. In *Protein Expression in Mammalian Cells: Methods and Protocols*; Springer: Berlin/Heidelberg, Germany, 2011; pp. 65–74.
8. Degors, I.M.; Wang, C.; Rehman, Z.U.; Zuhorn, I.S. Carriers break barriers in drug delivery: Endocytosis and endosomal escape of gene delivery vectors. *Acc. Chem. Res.* **2019**, *52*, 1750–1760. [CrossRef] [PubMed]
9. Rennick, J.J.; Johnston, A.P.; Parton, R.G. Key principles and methods for studying the endocytosis of biological and nanoparticle therapeutics. *Nat. Nanotechnol.* **2021**, *16*, 266–276. [CrossRef] [PubMed]
10. Kaźmierczak, Z.; Szostak-Paluch, K.; Przybyło, M.; Langner, M.; Witkiewicz, W.; Jędruchniewicz, N.; Dąbrowska, K. Endocytosis in cellular uptake of drug delivery vectors: Molecular aspects in drug development. *Bioorg. Med. Chem.* **2020**, *28*, 115556. [CrossRef] [PubMed]
11. Tu, Y.; Yu, A.C.H. Ultrasound-mediated drug delivery: Sonoporation mechanisms, biophysics, and critical factors. *BME Front.* **2022**, *2022*, 9807347. [CrossRef] [PubMed]
12. Sitta, J.; Howard, C.M. Applications of ultrasound-mediated drug delivery and gene therapy. *Int. J. Mol. Sci.* **2021**, *22*, 11491. [CrossRef] [PubMed]
13. Fan, Z.; Kumon, R.E.; Deng, C.X. Mechanisms of microbubble-facilitated sonoporation for drug and gene delivery. *Ther. Deliv.* **2014**, *5*, 467–486. [CrossRef] [PubMed]
14. Karthikesh, M.S.; Yang, X. The effect of ultrasound cavitation on endothelial cells. *Exp. Biol. Med.* **2021**, *246*, 758–770. [CrossRef]
15. Zhou, Y.; Yang, K.; Cui, J.; Ye, J.; Deng, C. Controlled permeation of cell membrane by single bubble acoustic cavitation. *J. Control. Release* **2012**, *157*, 103–111. [CrossRef] [PubMed]
16. Yoo, J.; Heo, D.; Hwang, Y.; Kim, C.; Park, B. Ultrasound-mediated membrane modulation for biomedical applications. *Nanomaterials* **2025**, *15*, 884. [CrossRef] [PubMed]
17. Wu, J.; Nyborg, W.L. Ultrasound, cavitation bubbles and their interaction with cells. *Adv. Drug Deliv. Rev.* **2008**, *60*, 1103–1116. [CrossRef] [PubMed]
18. Panje, C.M.; Wang, D.S.; Pysz, M.A.; Paulmurugan, R.; Ren, Y.; Tranquart, F.; Tian, L.; Willmann, J.K. Ultrasound-mediated gene delivery with cationic versus neutral microbubbles: Effect of DNA and microbubble dose on in vivo transfection efficiency. *Theranostics* **2012**, *2*, 1078. [CrossRef] [PubMed]
19. Fletcher, S.-M.P.; Zhang, Y.; Chisholm, A.; Martinez, S.; McDannold, N. The impact of pulse repetition frequency on microbubble activity and drug delivery during focused ultrasound-mediated blood-brain barrier opening. *Phys. Med. Biol.* **2024**, *69*, 145002.
20. Zhang, Y.; Tachibana, R.; Okamoto, A.; Azuma, T.; Sasaki, A.; Yoshinaka, K.; Tei, Y.; Takagi, S.; Matsumoto, Y. Ultrasound-mediated gene transfection in vitro: Effect of ultrasonic parameters on efficiency and cell viability. *Int. J. Hyperth.* **2012**, *28*, 290–299. [CrossRef]
21. Hughes, D.; Nyborg, W. Cell Disruption by Ultrasound: Streaming and other activity around sonically induced bubbles is a cause of damage to living cells. *Science* **1962**, *138*, 108–114. [PubMed]
22. Przystupski, D.; Ussowicz, M. Landscape of cellular bioeffects triggered by ultrasound-induced sonoporation. *Int. J. Mol. Sci.* **2022**, *23*, 11222. [CrossRef] [PubMed]
23. Duvshani-Eshet, M.; Machluf, M. Therapeutic ultrasound optimization for gene delivery: A key factor achieving nuclear DNA localization. *J. Control. Release* **2005**, *108*, 513–528. [CrossRef] [PubMed]
24. Hernot, S.; Klibanov, A.L. Microbubbles in ultrasound-triggered drug and gene delivery. *Adv. Drug Deliv. Rev.* **2008**, *60*, 1153–1166. [CrossRef] [PubMed]
25. Majumdar, S.; Chowdhury, S. Novel therapeutic application of microbubbles for targeted drug delivery. *Int. J. Pharma Bio Sci.* **2010**, *1*, 1–9.
26. Wei, H.; Liu, J.; Wang, W.; Qiu, C.; Hu, Z. Effect of diagnostic ultrasound at different mechanical indexes on microbubbles. *Int. J. Clin. Exp. Med.* **2019**, *12*, 12591–12597.
27. Cobbold, R.S. *Foundations of Biomedical Ultrasound*; Oxford University Press: Oxford, UK, 2006.
28. De Jong, N.; Emmer, M.; Van Wamel, A.; Versluis, M. Ultrasonic characterization of ultrasound contrast agents. *Med. Biol. Eng. Comput.* **2009**, *47*, 861–873. [CrossRef] [PubMed]
29. Wang, M.; Zhang, Y.; Cai, C.; Tu, J.; Guo, X.; Zhang, D. Sonoporation-induced cell membrane permeabilization and cytoskeleton disassembly at varied acoustic and microbubble-cell parameters. *Sci. Rep.* **2018**, *8*, 3885. [PubMed]

30. Helfield, B.; Chen, X.; Watkins, S.C.; Villanueva, F.S. Biophysical insight into mechanisms of sonoporation. *Proc. Natl. Acad. Sci. USA* **2016**, *113*, 9983–9988. [CrossRef] [PubMed]
31. Samuel, S.; Miller, D.L.; Fowlkes, J.B. The relationship of acoustic emission and pulse-repetition frequency in the detection of gas body stability and cell death. *Ultrasound Med. Biol.* **2006**, *32*, 439–447. [CrossRef] [PubMed]
32. Xu, S.; Zong, Y.; Feng, Y.; Liu, R.; Liu, X.; Hu, Y.; Han, S.; Wan, M. Dependence of pulsed focused ultrasound induced thrombolysis on duty cycle and cavitation bubble size distribution. *Ultrason. Sonochem.* **2015**, *22*, 160–166. [CrossRef] [PubMed]
33. Cochran, M.; Wheatley, M.A. In vitro gene delivery with ultrasound-triggered polymer microbubbles. *Ultrasound Med. Biol.* **2013**, *39*, 1102–1119. [CrossRef] [PubMed]
34. Karshafian, R.; Bevan, P.D.; Williams, R.; Samac, S.; Burns, P.N. Sonoporation by ultrasound-activated microbubble contrast agents: Effect of acoustic exposure parameters on cell membrane permeability and cell viability. *Ultrasound Med. Biol.* **2009**, *35*, 847–860. [CrossRef] [PubMed]
35. Qiu, Y.; Zhang, C.; Tu, J.; Zhang, D. Microbubble-induced sonoporation involved in ultrasound-mediated DNA transfection in vitro at low acoustic pressures. *J. Biomech.* **2012**, *45*, 1339–1345. [PubMed]
36. Qiu, Y.; Luo, Y.; Zhang, Y.; Cui, W.; Zhang, D.; Wu, J.; Zhang, J.; Tu, J. The correlation between acoustic cavitation and sonoporation involved in ultrasound-mediated DNA transfection with polyethylenimine (PEI) in vitro. *J. Control. Release* **2010**, *145*, 40–48. [CrossRef] [PubMed]
37. Li, Y.; Chen, Z.; Ge, S. Sonoporation: Underlying mechanisms and applications in cellular regulation. *Bio Integr.* **2021**, *2*, 29–36. [CrossRef]